RSC Advances

PAPER

View Article Online
View Journal | View Issue

Cite this: *RSC Adv.*, 2021, **11**, 39728

Design, synthesis, docking study and anticancer evaluation of new trimethoxyphenyl pyridine derivatives as tubulin inhibitors and apoptosis inducers†

Mohamed Hagras,[a] Asmaa A. Mandour,[b] Esraa A. Mohamed,[b] Eslam B. Elkaeed,[a] Ibrahim M. M. Gobaara,[c] Ahmed B. M. Mehany,[c] Nasser S. M. Ismail *[b] and Hanan M. Refaat[b]

Microtubules have become an appealing target for anticancer drug development including mainly colchicine binding site inhibitors (CBSIs). A new series of novel trimethoxypyridine derivatives were designed and synthesized as tubulin targeting agents. *In vitro* anti-proliferative activities of the tested compounds compared to colchicine against hepatocellular carcinoma (HepG-2), colorectal carcinoma (HCT-116), and breast cancer (MCF-7) was carried out. Most of compounds showed significant cytotoxic activities. Compounds **Vb**, **Vc**, **Vf**, **Vj** and **VI** showed superior anti-proliferative activities to colchicine. Where compound **VI** showed IC_{50} values of 4.83, 3.25 and 6.11 μM compared to colchicine (7.40, 9.32, 10.41 μM) against HCT 116, HepG-2 and MCF-7, respectively. The enzymatic activity against tubulin enzyme was carried out for the compounds that showed high anti-proliferative activity. Also, compound **VI** exhibited the highest tubulin polymerization inhibitory effect with an IC_{50} value of 8.92 nM compared to colchicine (IC_{50} value = 9.85 nM). Compounds **Vb**, **Vc**, **Vf**, **Vj**, & **VIIIb** showed promising activities with IC_{50} values of 22.41, 17.64, 20.39, 10.75, 31.86 nM, respectively. Cell cycle and apoptosis test for compound **VI** against HepG-2 cells, indicated that compound **VI** can arrest cell cycle at G2/M phase, and can cause apoptosis at pre-G1 phase, with high apoptotic effect 18.53%. Molecular docking studies of the designed compounds confirmed the essential hydrogen bonding with **CYS241** beside the hydrophobic interaction at the binding site compared to reference compounds which assisted in the prediction of the structure requirements for the detected antitumor activity.

Received 27th October 2021
Accepted 2nd December 2021

DOI: 10.1039/d1ra07922k

rsc.li/rsc-advances

1. Introduction

Microtubules are vital components in all eukaryotic cytoskeletons required for all cell functions. These tube-shaped filamentous protein polymers play important roles in cell signaling, intracellular transport, cell proliferation, cell division and mitosis, and that makes them an appealing target for anticancer drug development. Microtubules are comprised of two α- and β-tubulin heterodimer subunits in eukaryotic cells.[1–6] Microtubule targeting drugs generally can bind to one of three main sites on tubulin, the paclitaxel site, the vinca alkaloid and the colchicine binding sites.[5] Microtubules are characterized by being in a dynamic equilibrium of polymerization and depolymerization, that led to the development of tubulin polymerization inhibitors such as colchicine.[7] These are widely used for destroying various types of tumor cells *via* disturbing this equilibrium through the colchicine binding site in tubulin.[8–11]

Inhibitors that work by binding to either taxane or vinca alkaloid binding sites are of limited clinical use due to several disadvantages including structural complexity and low water solubility,[12] while colchicine binding site inhibitors (CBSIs) showed remarkable anti-proliferative activities in recent decades.[13] Microtubules as an anticancer target including CBSIs are believed to induce cell cycle arrest at G2/M and apoptosis which supports its anticancer activity.[14]

Nitrogenous heterocycles generally play an important role in drug discovery.[15] The pyridine scaffold was distinguished as tubulin targeting agents acting on colchicine binding site. Hereby pyridine nucleus specifically was assumed to form the essential hydrogen bond with **CYS241** in the colchicine binding site, thus it was believed that pyridine might be introduced into the structures of CBSIs.[1]

[a]*Pharmaceutical Organic Chemistry DepartmentFaculty of Pharmacy (Boys), Al-Azhar University, Cairo, Egypt*

[b]*Pharmaceutical Chemistry Department, Faculty of Pharmacy, Future University in Egypt (FUE), Cairo 11835, Egypt. E-mail: Nasser.saad@fue.edu.eg*

[c]*Zoology Department, Faculty of Science, Al-Azhar University, Cairo, Egypt*

† Electronic supplementary information (ESI) available. See DOI: 10.1039/d1ra07922k

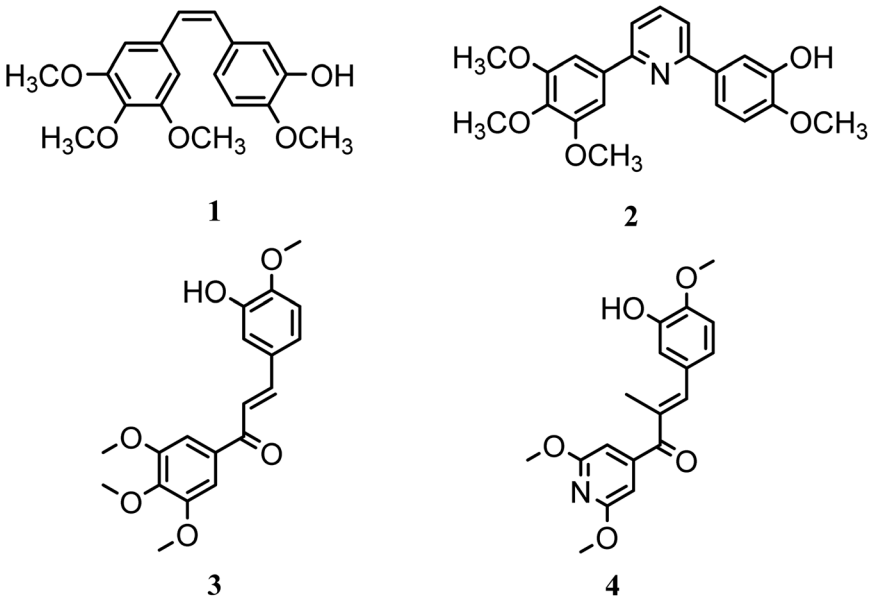

Fig. 1 Structures of compounds 1–4 acting as CBSIs.

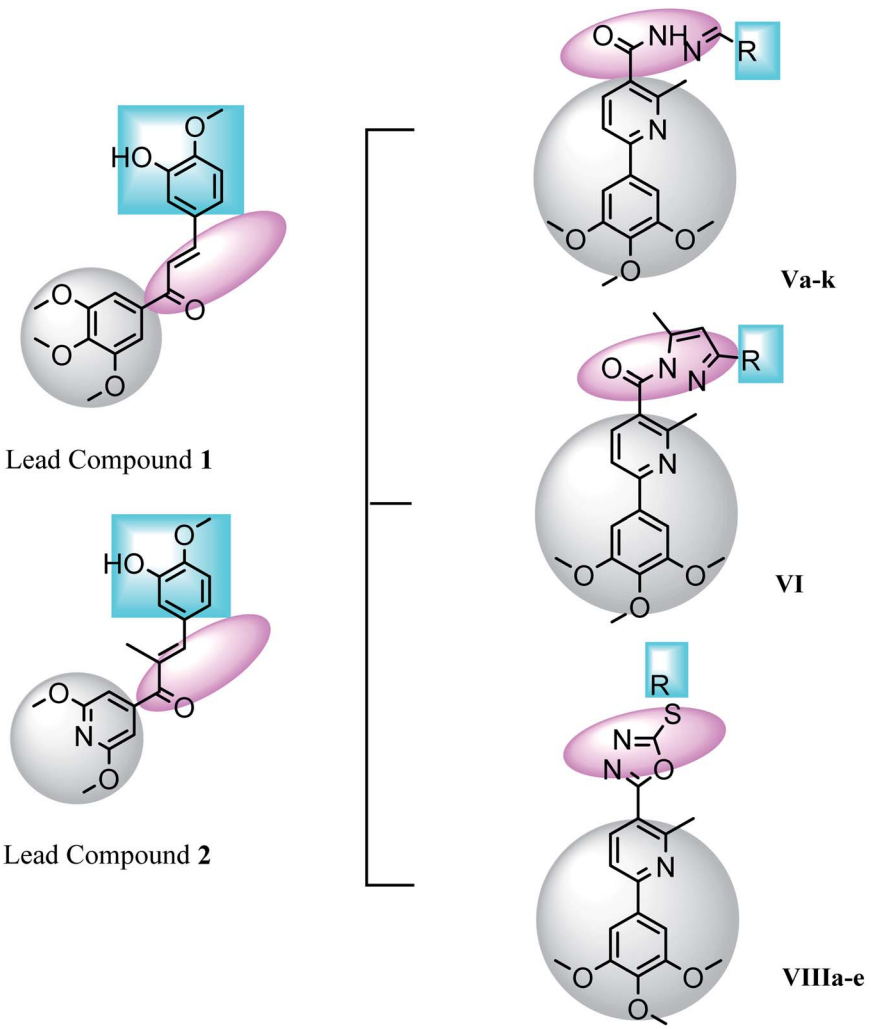

Fig. 2 Features' similarities of the lead compounds 3 & 4 and the designed compounds Va–k, VI & VIIIa–e as tubulin inhibitors.

In this study, a novel series of pyridine derivatives was designed and synthesized as anti-proliferative agents with tubulin targeting activity.[16] The design of this scaffold was focused on the exploration of the previous SAR of the colchicine binding site inhibitors (CBSIs)[1,17] (Fig. 1). Where trimethoxyphenyl pyridines have provided successful scaffolds as colchicine binding site inhibitors, several bioisosteric modifications was achieved while retaining the ability to bind in a similar or related manner to pyridine chalcone derivatives.

Combretastatin A-4 (**1**) (CA-4), a unique colchicine binding site inhibitor, was isolated from the African willow tree bark *Combretum caffrum*, showed potent antimitotic and vascular disrupting activities. Derivatives of CA-4 were developed as potential candidates for cancer therapy,[1,17–19] targeting colchicine binding site to block microtubule assembly, and cause cell death to the tumor.[17] As trimethoxyphenyl (TMP) moiety in CA-4 was critical for activity where the 4-methoxy group is responsible for the critical hydrogen bond with **CYS241**.[17,20–22] So, most derivatives with modified TMP moiety showed reduced anticancer potency.[23–26] However, it was reported that heterocyclic-fused pyrimidine compounds showed N-1 atom-hydrogen bond with **CYS241** residue, this demonstrated that quinoline or quinazoline moieties with N-1 atom can substitute the TMP moiety which is essential for hydrogen binding to the colchicine site showing improved anti-proliferative activity.[27] Also, the introduction of pyridine linker besides the TMP moiety was beneficial and showed reported compounds of potent anti-proliferative activity as in compound **2**.[17]

In this research a bioisosteric replacement of the two lead compounds **3** & **4**, besides a molecular docking study was performed to design novel TMP pyridine derivatives as CBSIs (Fig. 1).[1] The reported SAR was aligned with the newly synthesized structures and verified to bind with the same amino acids and the same binding mode as reference compounds.

1.1. Rationale design

Pyridine chalcone derivatives are very popular in the design of CBSIs. It not only binds to the hydrophobic pocket by hydrophobic interaction but also is responsible for hydrogen binding with **CYS241** residue.[1,17] That's why pyridine is proved to provide successful scaffolds for new CBSIs discovery.[1,17]

The design of the novel pyridine chalcone derivatives was based on the bioisosteric modifications and structure optimization of the two lead compounds **3**, **4** (Fig. 1),[1] according to the reported SAR and molecular modeling studies results. The trimethoxyphenyl moiety in lead compound **3** or the dimethoxy pyridine moiety in lead compound **4** was replaced by trimethoxyphenylpyridinyl moiety. While the replacement of the substituted phenyl moiety by alkyl or alkylthio or aryl moiety maintains the binding interactions. Besides, replacement of chalcone linker by hydrozoyl group in compounds **Va–k**, *N*-

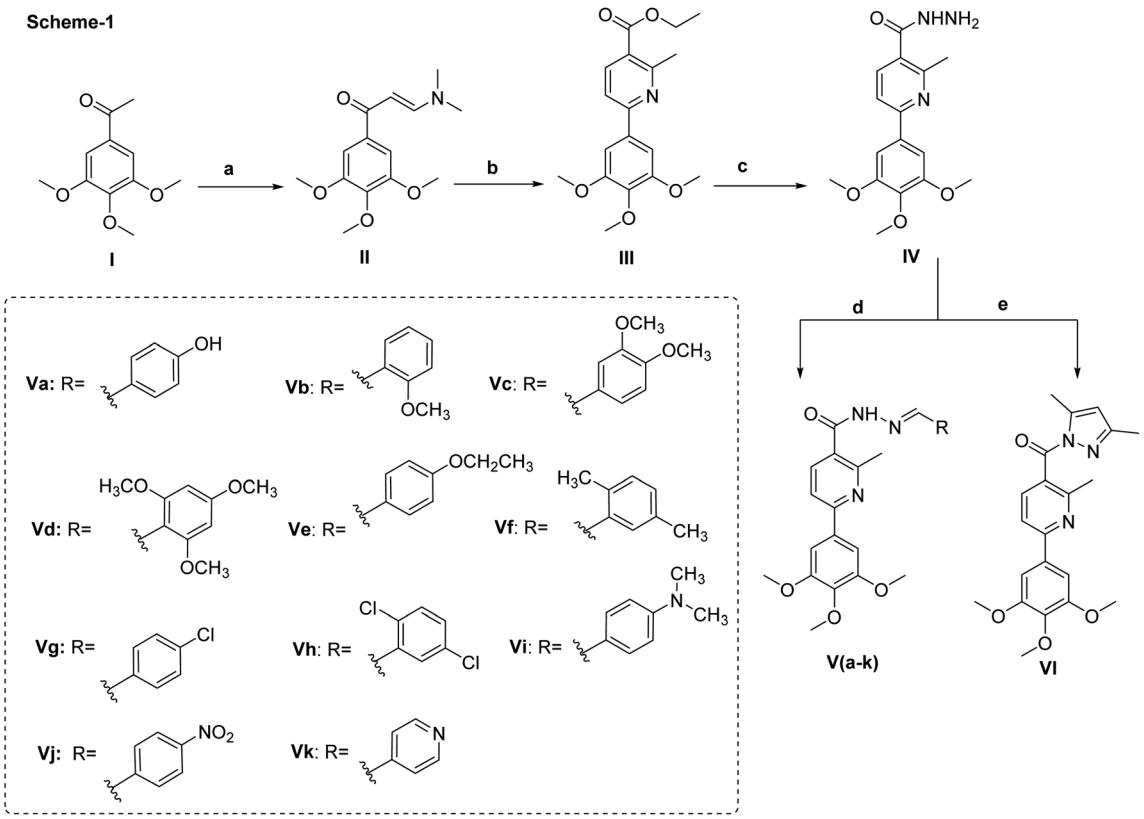

Scheme 1 Synthetic scheme of compounds II, III, IV, Va–k & VI. Reagents and conditions; (a) DMF-DMA/80 °C, 8 h. (b) Glacial acetic acid, ammonium acetate, ethyl acetoacetate, reflux, overnight. (c) Ethanol, hydrazine hydrate, reflux, 8 h. (d) Aldehyde, ethanol, glacial acetic acid, reflux, 8–12 h. (e) Acetyl acetone, glacial acetic acid, 100 °C, 7 h.

carbonyl pyrazole ring in compound **VI** and oxadiazole in compounds **VIIIa–e** maintains the same binding mode as reference compounds (Fig. 2).

2. Results and discussion

2.1. Chemistry

The key starting material **II** was prepared directly from 1-(3,4,5-trimethoxyphenyl)ethan-1-one and dimethylformamide-dimethylacetal (DMF-DMA) under solvent free conditions. The presence of two extra doublet signals in the spectrum of ^{1}H NMR at δ 8.08 and 5.92 with *J*-value of 12 Hz confirmed the chemical structure and the proposed *E*-configuration of compound **II**.

To access the desired pyridine-based scaffold, enaminone **II** was allowed to react with ethyl acetoacetate and ammonium acetate in glacial acetic acid to yield ethylesterpyridine **III**. The formation of pyridine ring was confirmed by the appearance of two doublet signals, each equal one proton, at δ 7.95 and 7.88, respectively. The isolated ethylester derivative **III** was then converted into the second key starting material acid hydrazide **IV** by allowing it to react with hydrazine hydrate.

Finally, the hydrazide intermediate **IV** was utilized to complete the series of optimized benzylidenenicotinohydrazide derivatives. Hence, the hydrazide derivative **IV** was allowed to react with eleven different benzaldehyde derivatives; to afford the corresponding final products (**Va–k**) (Scheme 1). The chemical structures of newly synthesized compounds were confirmed by their elemental and spectral data. For example, the ethoxy group of compound **III** was represented in the ^{1}H NMR spectrum by two signals at δ 4.35 and 1.38. These two characteristic signals were replaced with two broad singlets at δ 9.57 and δ 4.50 corresponding to NH and NH_2 respectively when treated with hydrazine hydrate (compound **IV**). In case of compounds (**Va–k**), the characteristic signal at δ 4.50 of NH_2 moieties was disappeared from the ^{1}H NMR spectra and replaced with singlet signal at approximately δ 8.42 ppm due to amidic proton, in addition to the presence of extra aromatic protons, equivalent, in each case, to the number of aromatic side chains connected with the terminal nitrogen.

Taken ^{1}H NMR spectrum of compound **Va** as a detailed example, it showed, in addition to the protons of trimethoxylphenylpyridine nucleus, two broad singlets each for one proton at δ 11.56 and 9.93 due to NH and OH respectively, two doublet signals each for two protons at δ 7.56 and 6.84 due hydroxybenzene ring and singlet signal at δ 8.19 corresponding to amidic proton. Also, the ^{13}C NMR spectrum of compound **Va** showed eighteen signals. Fifteen signals in the aromatic region from δ 164.18 to 104.20, and three signals in aliphatic part at δ 60.41, 56.55 and 23.25.

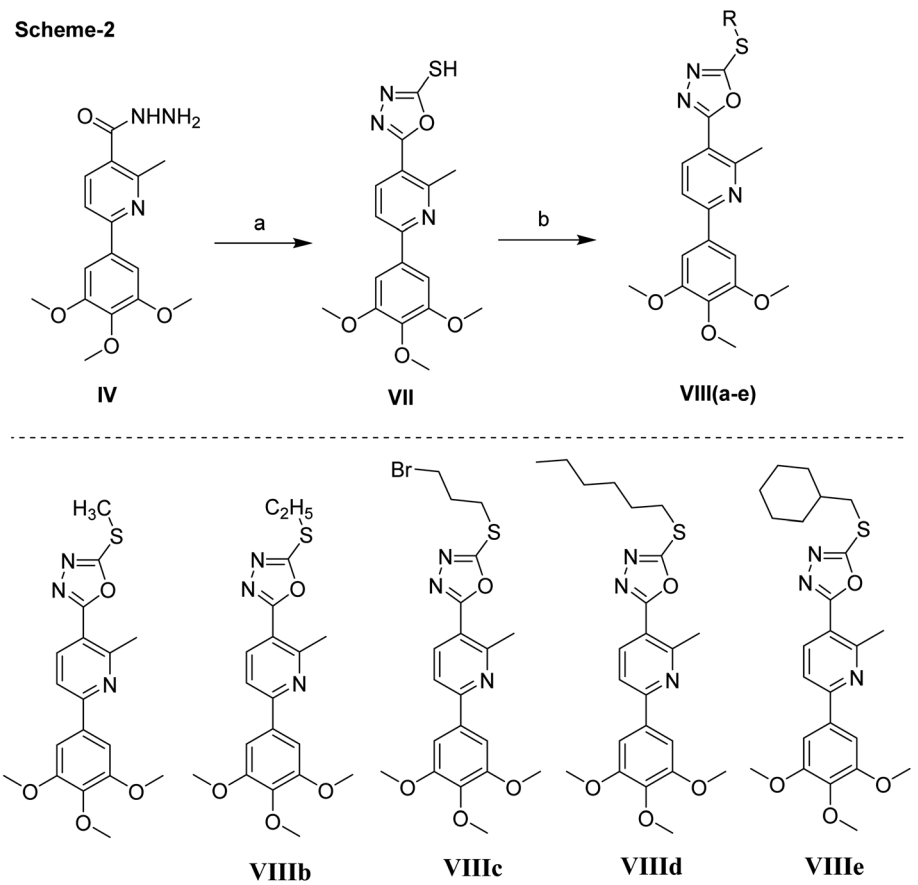

Scheme 2 Synthetic scheme of compounds VII & VIIIa–e. Reagents and conditions, (a) CS_2, KOH. (b) RX, NaOAc, EtOH, reflux, 2 h, 200 °C.

Table 1 *In vitro* anti-proliferative activities of the tested compounds and colchicine IC_{50} values

		In vitro anti-proliferative activities IC_{50}[a] (μM)		
No	Compound	HCT 116 IC_{50}	HEPG-2 IC_{50}	MCF-7 IC_{50}
1	**Va**	11.7 ± 0.28	15.37 ± 0.47	21.51 ± 0.67
2	**Vb**	**7.19 ± 0.2**	**6.55 ± 0.12**	**8.5 ± 0.24**
3	**Vc**	**6.45 ± 0.17**	**5.87 ± 0.11**	**9.15 ± 0.31**
4	**Vd**	10.75 ± 0.23	12.52 ± 0.35	15.8 ± 0.46
5	**Ve**	*25.17 ± 0.62*	*36.27 ± 0.82*	*46.6 ± 0.95*
6	**Vf**	**5.2 ± 0.08**	**6.51 ± 0.15**	**6.32 ± 0.14**
7	**Vg**	16.7 ± 0.55	22.37 ± 0.54	31.54 ± 0.7
8	**Vh**	21.19 ± 0.5	13.11 ± 0.37	30.05 ± 0.75
9	**Vi**	*30.25 ± 0.75*	*40.08 ± 0.95*	*50.13 ± 0.83*
10	**Vj**	**4.5 ± 0.05**	**3.74 ± 0.03**	**4.82 ± 0.05**
11	**Vk**	13.26 ± 0.35	10.81 ± 0.28	17.53 ± 0.57
12	**VI**	**4.83 ± 0.06**	**3.25 ± 0.05**	**6.11 ± 0.17**
13	**VIIIa**	14.1 ± 0.38	13.45 ± 0.36	18.23 ± 0.55
14	**VIIIb**	9.74 ± 0.21	8.57 ± 0.25	14.85 ± 0.37
15	**VIIIc**	20.45 ± 0.65	19.31 ± 0.64	25.16 ± 0.64
16	**VIIId**	15.34 ± 0.48	12.74 ± 0.31	27.18 ± 0.68
17	**VIIIe**	17.38 ± 0.47	15.67 ± 0.45	21.37 ± 0.45
	Colchicine	**7.40 ± 0.2**	**9.32 ± 0.2**	**10.41 ± 0.3**

[a] IC_{50} values are the mean ± SD of three separate experiments.

Table 2 *In vitro* tubulin polymerization inhibition results

No.	Compound	IC_{50} nM ml^{-1}
1	**Vb**	22.41
2	**Vc**	17.64
3	**Vd**	50.11
4	**Vf**	20.39
5	**Vj**	10.75
6	**Vk**	43.16
7	**VI**	**8.92**
8	**VIIIa**	64.13
9	**VIIIb**	31.86
10	**VIIId**	48.27
	Colchicine	9.85

Next, the synthesis of the 1,3,4-oxadiazolyl scaffold was achieved starting from the acid hydrazide **IV** and carbon disulfide in an alcoholic potassium hydroxide solution according to Hoggarth's approach,[28] followed by alkylation of the thiol group to afford the 2-alkyllmercaptyl derivatives (**VIIIa–e**). The structures of this set of new compounds were confirmed by their elemental and spectral analyses data as detailed in the experimental section. ^{1}H NMR spectra characteristic by the presence of extra aliphatic protons, equivalent, in each case, to the number of aliphatic side chains connected with the sulphur atom. These observations, collectively, confirm tethering the

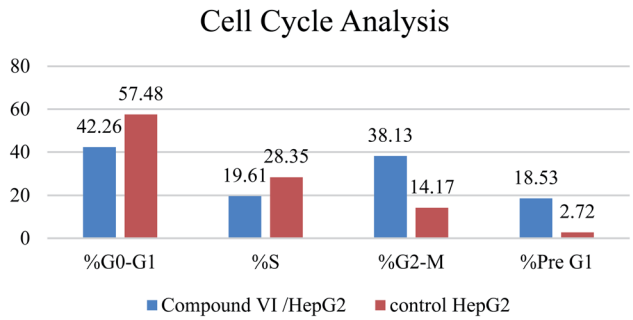

Fig. 3 Effect of compound VI on cell cycle progression in HepG-2 cells.

alkyl moiety with the oxadiazole position-2. Taken ^{1}H NMR spectrum of compound **VIIIa** as a detailed example, it showed, in addition to the protons of main aromatic core, a singlet signal equivalent to three protons at δ 2.87 due to methyl group. The ^{13}C NMR spectrum of compound **VIIIa** showed fifteen signals (Scheme 2).

2.2. Biological evaluation

2.2.1. *In vitro* anti-proliferative activity. The *in vitro* cytotoxic activities of the synthesized compounds were estimated using MTT method.[29–32] The test used human cancer cell lines including colorectal carcinoma (HCT-116), hepatocellular carcinoma (HepG-2), and breast cancer (MCF-7). Anti-proliferative activity was represented in IC_{50} values (Table 1). The cytotoxic screening revealed that the studied compounds had varying degrees of activity showing successful anticancer candidates with promising anticancer activity against the studied cells. Results were compared to colchicine (IC_{50} = 7.40, 9.32, and 10.41 μM against HCT116, HepG-2, and MCF-7, respectively), where compounds **Vb**, **Vc**, **Vf**, **Vj** and **VI** showed potent cytotoxic activities with IC_{50} values ranging from 3.25 to 9.15 μM against the three mentioned cell lines. Both compounds **Vj** and **VI** showed the best superior IC_{50} results than colchicine, where compound **Vj** showed 4.5, 3.74 and 4.82 μM, and compound **VI** showed 4.83, 3.25 and 6.11 μM against HCT 116, HEPG-2 and MCF-7, respectively. In addition, compound **VIIIb** exhibited superior activity against HEPG-2 with IC_{50} value of 8.57 μM. Additionally, compounds **Va**, **Vd**, **Vg**, **Vh**, **Vk**, **VIIIa**, **VIIIc**, **VIIId** and **VIIIe** displayed moderate anti-proliferative activities against all the tested cell lines with IC_{50} values ranging from 10.75 to 31.54 μM (Table 1).

2.2.2. Tubulin polymerization assay. The inhibitory effect of the most active anti-proliferative members was also tested for tubulin polymerization inhibition. Using a fluorescent plate reader, the inhibition assay on microtubule polymerization was

Table 3 Effect of compound VI on cell cycle progression in HepG-2 cells

		% G0–G1	% *S*	% G2-M	% Pre G1	Comment
1	Compound **VI**/HepG2	42.26	19.61	38.13	18.53	Cell cycle arrest at G2/M
2	Control HepG2	57.48	28.35	14.17	2.72	

Table 4 The apoptotic effect of compound VI

		Apoptosis			
		Total	Early	Late	Necrosis
1	Compound **VI**/HepG2	18.53	6.9	9.24	2.39
2	Control HePG2	2.72	0.55	0.63	1.54

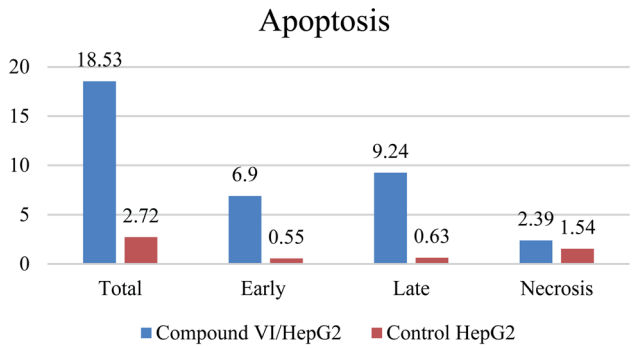

Fig. 4 The apoptotic effect of compound VI.

turbidimetrically assessed.[33] Colchicine was used as positive control. Compound **VI** exhibited the highest tubulin polymerization inhibitory effect with IC_{50} value = 8.92 nM. The result was more potent than that of colchicine (IC_{50} = 9.85 nM) (Table 2). Moreover, compounds **Vb**, **Vc**, **Vf**, **Vj**, & **VIIIb** showed promising activities with IC_{50} values of 22.41, 17.64, 20.39, 10.75, 31.86 nmol L^{-1}, respectively. Compounds **Vd**, **Vk**, **VIIIa** & **VIIId** showed moderate activity with IC_{50} values of 50.11, 43.16, 64.13 and 48.27 nM mL^{-1} respectively.

2.2.3. Cell cycle analysis. The effect of compound **VI**, that showed the most promising *in vitro* inhibitory results, on cell cycle distribution was investigated. The inhibitory effect on cancer cell growth was better understood as a result of this study. In this experiment, HepG-2 cells were used.[34–37] HepG-2 cells were treated for 24 h with compound **VI** at a concentration corresponding to its IC_{50} value (3.25 μM). The results revealed that compound **VI** induced a decrease in HepG-2 cells percentage from 28.35% to 19.61% at *S* phase. It showed marked increase in the percentage of HepG-2 cells from 14.17% to 38.13% at G2/M phase. Also, the percentage of HepG-2 cells increased from 2.72% to 18.53% at Pre-G1 phase. On the other hand, it decreased the percentage of HepG-2 cells at G0–G1 phase from 57.48% to 42.26%. These results indicated that compound **VI** can arrest G2/M phase in the cell cycle and can cause apoptosis at pre-G1 phase (Table 3 and Fig. 3).

2.2.4. Annexin V-FITC apoptosis assay. The proposed apoptotic effect of the compound **VI** was investigated using an annexin V and PI double staining assay.[38–40] Compound **VI** was tested against HepG-2 cells as a representative example. In this test, HepG-2 cells were incubated with compound **VI** at a concentration of (3.25 μM) for 24 h Table 4 and Fig. 4, 5 showed that compound **VI** induced apoptosis by 18.53% (6.9 and 9.24 at early and late apoptosis, respectively), which was thirteen times more than the standard control (1.39%).

2.3. Molecular modeling study

Molecular docking study was carried out using Libdock protocol in Discovery Studio 4.0 Software, where the prepared ten compounds with high *in vitro* tubulin polymerization inhibition results were docked into the colchicine binding site of tubulin. The binding mode of the designed compounds was studied to explain their biological results and to determine the essential

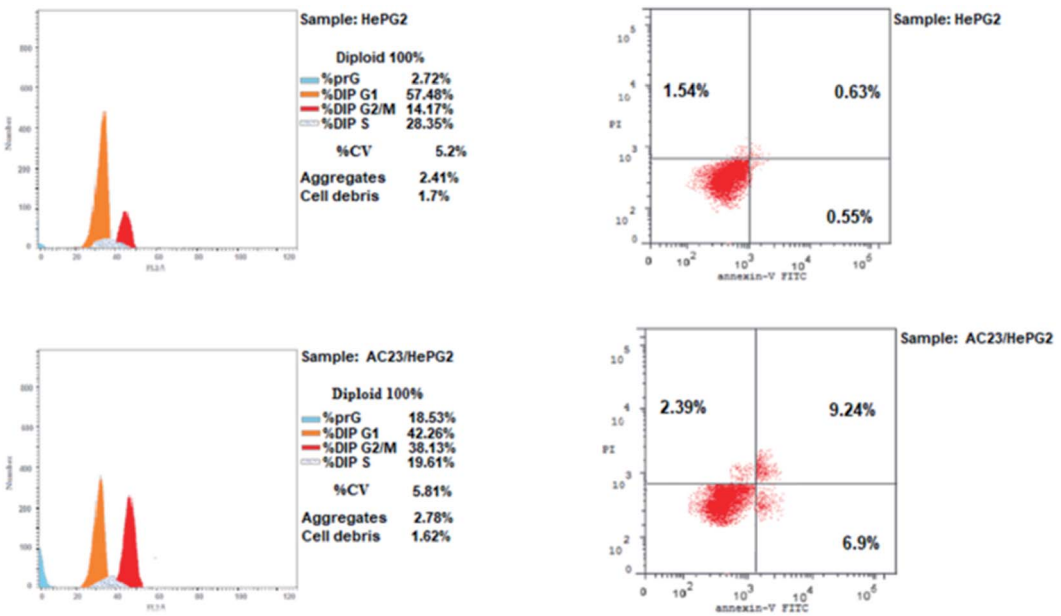

Fig. 5 HepG-2 cells distribution upon treatment with compound VI.

Table 5 The Libdock interaction energy of some newly synthesized compounds

Compound ID	Interaction diagram	Binding mode with tubulin	Libdock interaction energy (K cal mol^{-1})
Ref. comp. **3**	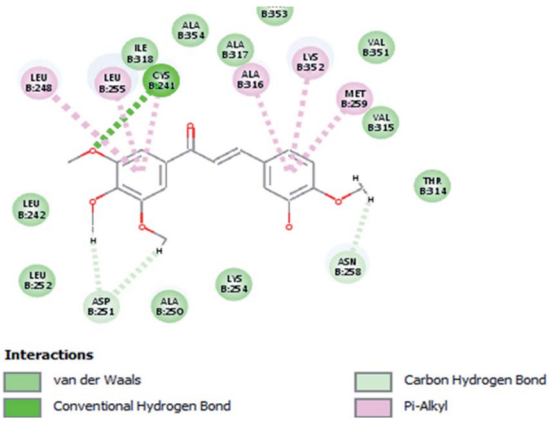	**CYS241**	−102
Ref. comp. **4**	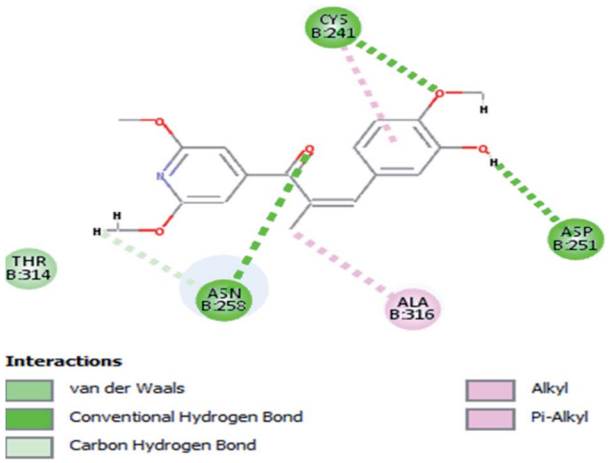	**CYS241**	−97
Vb	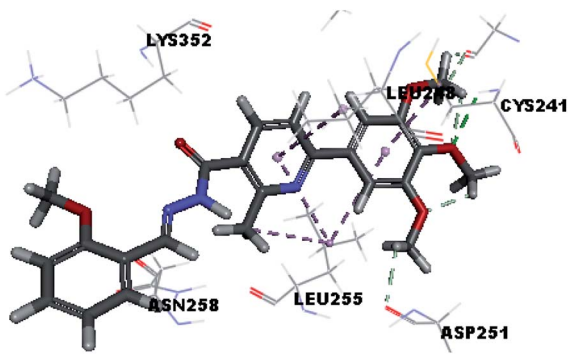	**CYS241**	−96.3

Table 5 (*Contd.*)

Compound ID	Interaction diagram	Binding mode with tubulin	Libdock interaction energy (K cal mol^{-1})
Vc	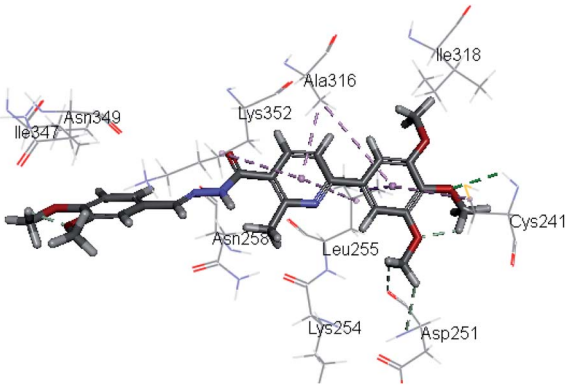	**CYS241**	−87.5
Vd	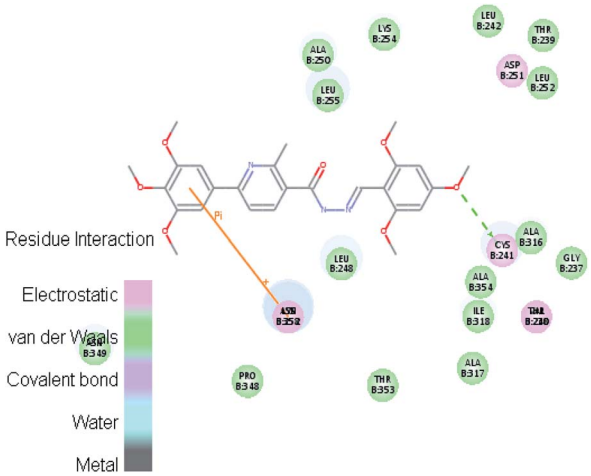	**CYS241**	−81.3
Vf	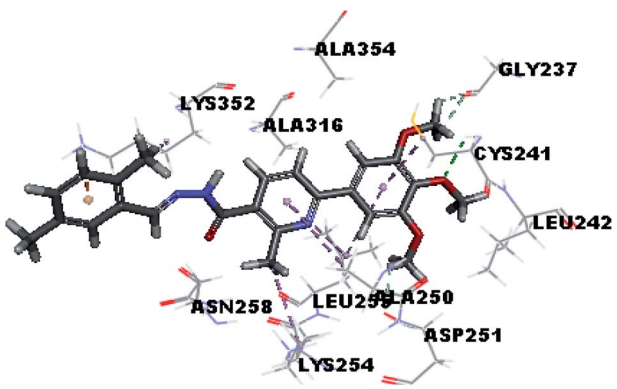	**CYS241**	−98.71

Table 5 (*Contd.*)

Compound ID	Interaction diagram	Binding mode with tubulin	Libdock interaction energy (K cal mol^{-1})
Vj	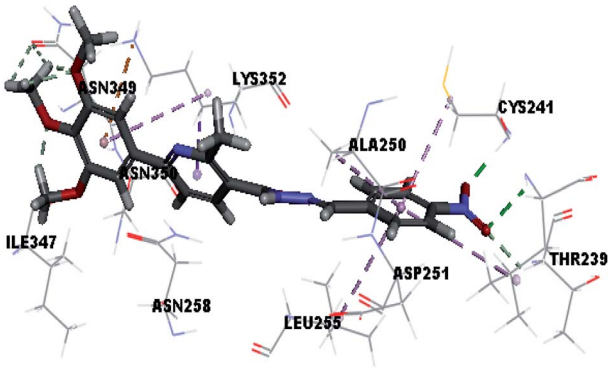	**CYS241**	−105.8
Vk	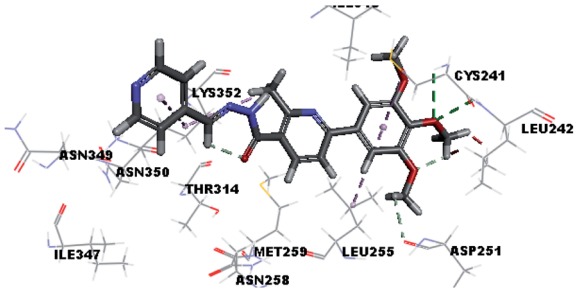	**CYS241**	−94.6
VI	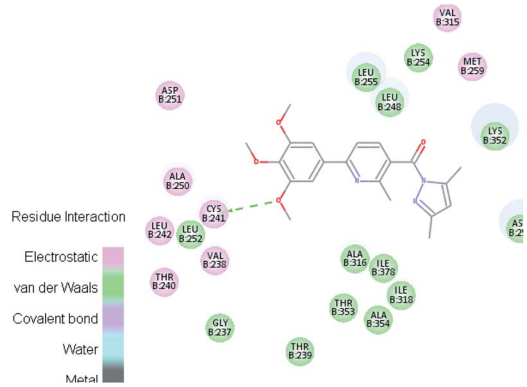	**CYS241**	−104.95
VIIIa	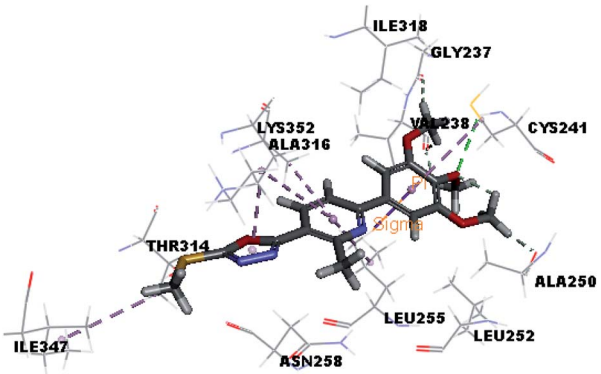	**CYS241**	−91.5

Table 5 (*Contd.*)

Compound ID	Interaction diagram	Binding mode with tubulin	Libdock interaction energy (K cal mol^{-1})
VIIIb	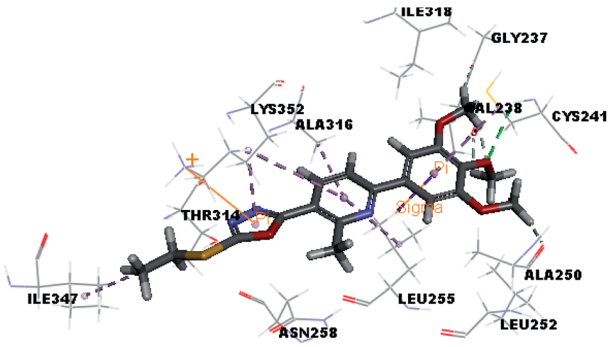	**CYS241**	−95.2
VIIId	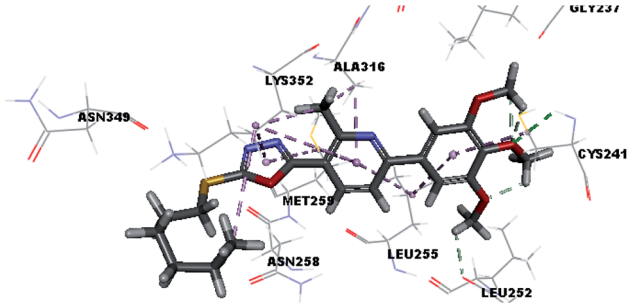	**CYS241**	−97.33

pharmacophoric features of the new compounds. The X-ray crystallographic enzyme tubulin complex with colchicine (PDB ID: 4O2B),[41] showed the presence of an essential hydrogen bond with **CYS241**, in addition to hydrophobic interaction. The selected pose of the new compounds out of ten poses that showed similarity to the binding mode compared to the two reference ligands is considered the best pose. Re-docking of the lead compounds was performed in the active site to confirm validation of docking protocol, which showed good results with RMSD value = 0.5 Å. The presented docking study showed similar binding mode between the lead compounds and the docked molecules. The binding mode and the interaction energy of the biologically active synthesized compounds are summarized in Table 5.

Where the molecular docking of the new compounds revealed that compounds **Vb**, **Vc**, **Vd**, **Vf**, **Vj**, **Vk**, **VI**, **VIIIb**, **VIIIc** and **VIIId** retained the essential H-bond with **CYS241** compared to reference compounds **3** and **4**. Compounds **Vj** & **VI** showed the highest interaction energy (E = **−105.8**, **−104.95**, respectively) compared to lead compounds **3** & **4.** The results were in consistence with the *in vitro* activity results of compounds **Vj** & **VI** which showed the highest inhibitory activity against tubulin compared to colchicine. It was observed too that compounds **Vb**, **Vc**, **Vf**, **Vj**, **VI** and **VIIIb** showed the same binding mode with good docking score values (Table 5).

These results explained that the substitution of *N*-carbonyl pyrazole ring as a linker moiety in compound **VI** is responsible for the hydrophobic interaction in addition to the trimethoxy phenyl essential HBA bond with **CYS241** showing a similar mode interaction to reference compounds.

3. Conclusion

A series of pyridine-based derivatives were designed, synthesized and evaluated for their *in vitro* tubulin inhibitory activity as well as their anti-proliferative activity against colorectal carcinoma (HCT-116), hepatocellular carcinoma (HepG-2), and breast cancer (MCF-7). Most of the novel trimethoxyphenyl pyridine derivatives exhibited significant cytotoxicity and tubulin inhibition activity.

Compound **VI** showed high interaction energy (E = **−104.95**), with the highest tubulin polymerization inhibitory effect of IC_{50} value = 8.92 nM. It also revealed potent anti-proliferative activity of IC_{50} 4.83, 3.25 and 6.11 μM against HCT 116, HEPG-2 and MCF-7, respectively. Compound **VI** can arrest the cell cycle at G2/M phase and can cause apoptosis at pre-G1 phase.

4. Materials and methods

4.1. Chemistry

4.1.1. General. ^{1}H NMR spectra were run at 400 MHz and ^{13}C spectra were determined at 100 MHz in deuterated dimethyl sulfoxide (DMSO-d_6) on a Varian Mercury VX-400 NMR spectrometer. Chemical shifts are given on the delta (δ) scale in parts per million (ppm). Chemical shifts were calibrated relative to

those of the solvents. Progress of reactions was monitored with Merck silica gel plates (IB2-F, 0.25 mm thickness). The infrared spectra were recorded in KBr disks on Pye Unicam SP 3300 and Shimadzu FT IR 8101 PC infrared spectrophotometer at Faculty of Pharmacy-Ain Shams University. Mass spectra were recorded on Hewlett Packard 5988 spectrometer at Regional Center for Mycology and Biotechnology, Al-Azhar University. Elemental analyses were performed on a Thermo Scientific Flash 2000 elemental analyzer at the Regional Center for Mycology and Biotechnology, Al-Azhar University. Melting points were determined using capillary tubes with a Stuart SMP30 apparatus and are uncorrected.

4.1.2. (*E*)-3-(Dimethylamino)-1-(3,4,5-trimethoxyphenyl) prop-2-en-1-one (II). To 1-(3,4,5-trimethoxyphenyl)ethan-1-one (3.2 g, 15.2 mmol) **I**, DMF-DMA (4.1 mL, 3.6 g, 30.4 mmol) was added and the reaction mixture was heated at 80 °C for 8 h. After cooling, the formed solid was collected by filtration, washed with petroleum ether and crystallized from ethanol to yield the desired product as a yellow solid (3.6 g, 90%) mp = 139 °C. ^{1}H NMR (400 MHz, DMSO) δ: 8.08 (d, J = 12 Hz, 1H), 7.41 (s, 2H), 5.92 (d, J = 12 Hz, 1H), 4.18 (s, 6H), 4.14 (s, 3H), 3.21 (s, 3H), 2.97 (s, 3H); MS (*m*/*z*) 265 (Scheme 1).

4.1.3. Ethyl 2-methyl-6-(3,4,5-trimethoxyphenyl)nicotinate (III). To a solution of the enaminone **II** (3.2 g, 12 mmol) in glacial acetic acid (35 mL), ethyl acetoacetate (8.4 g, 8.6 mL, 84 mmol) and ammonium acetate (9.24 g, 120 mmol) were added. The reaction mixture was heated under reflux overnight. The residue obtained after cooling and pouring into ice-water, was filtered and washed with petroleum ether then with water and finally crystallized from ethanol. Light green solid (3.43 g, 85%) mp = 110 °C; ^{1}H NMR (400 MHz, DMSO) δ: 7.95 (d, J = 8 Hz, 1H), 7.88 (d, J = 8 Hz, 1H), 7.38 (s, 2H), 4.35 (q, J = 8 Hz, 2H), 3.96 (s, 6H), 3.85 (s, 3H), 2.63 (s, 3H), 1.38 (t, J = 8 Hz, 3H); MS (*m*/*z*) 331 (Scheme 1).

4.1.4. 2-Methyl-6-(3,4,5-trimethoxyphenyl) nicotinohydrazide (IV). To a solution of **III** (3.3 g, 10 mmol) in ethanol (50 mL), hydrazine hydrate (99%, 2.5 mL, 47 mmol) was added dropwise. The reaction mixture was heated at reflux for 8 h then allowed to cool down to room temperature. The formed solid was filtered and crystallized from ethanol to give the desired product as white crystals (2.9 g, 92%) mp = 107 °C; ^{1}H NMR (400 MHz, DMSO) δ: 9.57 (brs, 1H), 7.87 (d, J = 8 Hz, 1H), 7.74 (d, J = 8 Hz, 1H), 7.38 (s, 2H), 4.50 (brs, 2H), 3.86 (s, 6H), 3.70 (s, 3H), 2.58 (s, 3H); MS (*m*/*z*) 317 (Scheme 1).

4.1.5. General procedure for synthesis of compounds (Va–k). To a solution of **IV** (0.2 g, 0.6 mmol) in 20 mL absolute ethanol, benzaldehyde derivative (0.6 mmol) was added with glacial acetic acid in catalytic amount and the mixture was heated under reflux for 8–12 h. The reaction mixture was concentrated and allowed to cool. The separated solid was filtered and crystallized from ethanol (Scheme 1).

*4.1.5.1. (E)-N′-(4-Hydroxybenzylidene)-2-methyl-6-(3,4,5-trimethoxyphenyl)nicotinohydrazide (**Va**).* Light yellow solid (0.19 g – 71%) mp = 240 °C; IR (KBr) cm^{-1}: 3435 (OH), 3300 (NH), 3075 (CH aromatic), 2922 (CH aliphatic), 1685 (C=O amide), 1633 (C=N); ^{1}H NMR (400 MHz, DMSO-d_6) δ: 11.56 (brs, 1H), 9.93 (brs, 1H), 8.19 (s, 1H), 7.95 (d, J = 8 Hz, 1H), 7.90 (d, J = 8 Hz, 1H), 7.56 (d, J = 8 Hz, 2H), 7.42 (s, 2H), 6.84 (d, J = 8 Hz, 2H), 3.87 (s, 6H), 3.71 (s, 3H), 2.60 (s, 1H). ^{13}C NMR (100 MHz, DMSO) δ: 164.18, 159.95, 156.15, 156.02, 153.60, 148.39, 139.32, 137.02, 133.84, 129.37, 128.61, 125.58, 117.40, 116.14, 104.20, 60.41, 56.55, 23.25; MS (*m*/*z*) 421; anal. calc. for: ($C_{23}H_{23}N_3O_5$, M_{wt} = 421): C, 65.55; H, 5.50; N, 9.97; found: C, 65.71; H, 5.73; N, 10.52%.

*4.1.5.2. (E)-N′-(2-Methoxybenzylidene)-2-methyl-6-(3,4,5-trimethoxyphenyl)nicotinohydrazide (**Vb**).* White solid (0.23 g – 82%) mp = 200 °C; IR (KBr) cm^{-1}: 3293 (NH), 3089 (CH aromatic), 2954 (CH aliphatic), 1685 (C=O amide), 1638 (C=N); ^{1}H NMR (400 MHz, DMSO-d_6) δ: 11.85 (brs, 1H), 8.42 (s, 1H), 7.94 (d, J = 8 Hz, 1H), 7.88 (d, J = 8 Hz, 1H), 7.80 (d, J = 8 Hz, 1H), 7.43 (s, 2H), 7.11 (d, J = 8 Hz, 1H), 7.05 (t, J = 8 Hz, 1H), 6.85 (t, J = 8 Hz, 1H), 3.87 (s, 6H), 3.84 (s, 3H), 3.71 (s, 3H), 2.64 (s, 1H). ^{13}C NMR (100 MHz, DMSO) δ: 164.60, 159.40, 157.98, 155.93, 153.49, 148.91, 144.13, 139.24, 136.80, 133.33, 131.60, 126.01, 122.54, 120.82, 117.36, 112.15, 104.51, 60.41, 56.96, 56.24, 23.25; MS (*m*/*z*) 435; anal. calc. for: ($C_{24}H_{25}N_3O_5$, M_{wt} = 435): C, 66.19; H, 5.79; N, 9.65; found: C, 65.87; H, 5.96; N, 9.65%.

*4.1.5.3. (E)-N′-(3,4-Dimethoxybenzylidene)-2-methyl-6-(3,4,5-trimethoxyphenyl)nicotinohydrazide (**Vc**).* White solid (0.25 g – 86%) mp = 205 °C; IR (KBr) cm^{-1}: 3288 (NH), 3010 (CH aromatic), 2925 (CH aliphatic), 1682 (C=O amide), 1638 (C=N); ^{1}H NMR (400 MHz, DMSO-d_6) δ: 11.57 (brs, 1H), 8.22 (s, 1H), 7.96 (d, J = 8 Hz, 1H), 7.91 (d, J = 8 Hz, 1H), 7.42 (s, 2H), 7.34 (s, 1H), 7.21 (d, J = 8 Hz, 1H), 7.03 (d, J = 8 Hz, 1H), 3.87 (s, 6H), 3.81 (s, 3H), 3.80 (s, 3H), 3.71 (s, 3H), 2.63 (s, 1H). ^{13}C NMR (100 MHz, DMSO) δ: 169.08, 164.60, 163.89, 155.94, 153.10, 149.32, 148.61, 142.39, 137.12, 132.30, 129.17, 126.71, 122.54, 117.74, 111.44, 108.69, 104.51, 60.53, 56.46, 56.03, 55.92, 23.64; MS (*m*/*z*) 465; anal. calc. for: ($C_{25}H_{27}N_3O_6$, M_{wt} = 465): C, 64.51; H, 5.85; N, 9.03; found: C, 64.78; H, 6.03; N, 9.17%.

*4.1.5.4. (E)-2-Methyl-N′-(2,4,6-trimethoxybenzylidene)-6-(3,4,5-trimethoxyphenyl)nicotinohydrazide (**Vd**).* Yellowish white solid (0.24 g – 77%) mp = 227 °C; IR (KBr) cm^{-1}: 3309 (NH), 3122 (CH aromatic), 2900 (CH aliphatic), 1665 (C=O amide), 1633 (C=N); ^{1}H NMR (400 MHz, DMSO-d_6) δ: 11.53 (brs, 1H), 8.20 (s, 1H), 7.91 (d, J = 8 Hz, 1H), 7.86 (d, J = 8 Hz, 1H), 7.38 (s, 2H), 6.28 (s, 2H), 3.87 (s, 6H), 3.86 (s, 3H), 3.79 (s, 3H), 3.63 (s, 6H), 2.60 (s, 1H). ^{13}C NMR (100 MHz, DMSO) δ: 170.18, 162.75, 162.63, 160.51, 159.86, 155.21, 153.69, 144.23, 139.84, 139.05, 130.19, 117.04, 104.47, 104.19, 91.68, 60.54, 56.37, 56.14, 55.81, 23.62; MS (*m*/*z*) 495; anal. calc. for: ($C_{26}H_{29}N_3O_7$, M_{wt} = 495): C, 63.02; H, 5.90; N, 8.48; O, 22.60; found: C, 62.89; H, 6.14; N, 8.65%.

*4.1.5.5. (E)-N′-(4-Ethoxybenzylidene)-2-methyl-6-(3,4,5-trimethoxyphenyl)nicotinohydrazide (**Ve**).* White solid (0.24 g – 86%) mp = 207 °C; IR (KBr) cm^{-1}: 3295 (NH), 3082 (CH aromatic), 2925 (CH aliphatic), 1675 (C=O amide), 1628 (C=N); ^{1}H NMR (400 MHz, DMSO-d_6) δ: 11.73 (brs, 1H), 8.24 (s, 1H), 7.96 (d, J = 8 Hz, 1H), 7.91 (d, J = 8 Hz, 1H), 7.66 (d, J = 8 Hz, 2H), 7.42 (s, 2H), 7.0 (d, J = 8 Hz, 2H), 4.1 (q, J = 8 Hz, 2H), 3.87 (s, 6H), 3.71 (s, 3H), 2.63 (s, 1H), 1.35 (t, J = 8 Hz, 3H). ^{13}C NMR (100 MHz, DMSO) δ: 168.06, 159.01, 156.96, 153.80, 148.92, 154.46, 141.69, 138.94, 137.51, 130.18, 128.14, 126.02, 118.76,

112.15, 103.50, 63.88, 60.72, 56.25, 23.25, 14.59; MS (*m*/*z*) 449; anal. calc. for: ($C_{25}H_{27}N_3O_5$, M_{wt} = 449): C, 66.80; H, 6.05; N, 9.35; found: C, 66.72; H, 6.23; N, 9.54%.

*4.1.5.6. (E)-N′-(2,5-Dimethylbenzylidene)-2-methyl-6-(3,4,5-trimethoxyphenyl)nicotinohydrazide (**Vf**).* Yellowish white solid (0.19 gm – 73%) mp = 206 °C; IR (KBr) cm^{-1}: 3295 (NH), 3080 (CH aromatic), 2900 (CH aliphatic), 1688 (C=O amide), 1631 (C=N); ^{1}H NMR (400 MHz, DMSO-d_6) δ: 11.79 (brs, 1H), 8.56 (s, 1H), 7.94 (d, J = 8 Hz, 1H), 7.90 (d, J = 8 Hz, 1H), 7.67 (s, 1H), 7.43 (s, 2H), 7.13 (s, 2H), 3.88 (s, 6H), 3.71 (s, 3H), 2.64 (s, 1H), 2.36 (s, 3H), 2.31 (s, 3H). ^{13}C NMR (100 MHz, DMSO) δ: 164.20, 162.88, 161.13, 160.42, 153.81, 150.02, 144.75, 142.0, 138.92, 137.12, 132.63, 131.92, 129.16, 124.99, 121.52, 117.35, 111.84, 60.42, 56.56, 56.03, 23.64, 21.83, 19.08; MS (*m*/*z*) 433; anal. calc. for: ($C_{25}H_{27}N_3O_4$, M_{wt} = 433): C, 69.27; H, 6.28; N, 9.69; found: C, 69.15; H, 6.47; N, 9.85%.

*4.1.5.7. (E)-N′-(4-Chlorobenzylidene)-2-methyl-6-(3,4,5-trimethoxyphenyl)nicotinohydrazide (**Vg**).* Light yellow solid (0.2 g – 74%) mp = 212 °C; IR (KBr) cm^{-1}: 3261 (NH), 3071 (CH aromatic), 2944 (CH aliphatic), 1681 (C=O amide), 1630 (C=N); ^{1}H NMR (400 MHz, DMSO-d_6) δ: 11.94 (brs, 1H), 8.28 (s, 1H), 7.97 (d, J = 8 Hz, 1H), 7.93 (d, J = 8 Hz, 1H), 7.76 (d, J = 8 Hz, 2H), 7.53 (d, J = 8 Hz, 2H), 7.42 (s, 2H), 3.87 (s, 6H), 3.71 (s, 3H), 2.63 (s, 1H). ^{13}C NMR (100 MHz, DMSO) δ: 164.21, 159.71, 158.69, 153.49, 148.60, 145.15, 139.24, 136.09, 130.89, 129.15, 122.55, 118.06, 112.15, 106.25, 104.83, 60.73, 56.24, 23.25; MS (*m*/*z*): 441 (0.37%, M + 2), 439 (0.9%, M^+); anal. calc. for: ($C_{23}H_{22}ClN_3O_4$, M_{wt} = 439): C, 62.80; H, 5.04; N, 8.06; found: C, 63.04; H, 5.11; N, 8.18%.

*4.1.5.8. (E)-N′-(2,5-Dichlorobenzylidene)-2-methyl-6-(3,4,5-trimethoxyphenyl)nicotinohydrazide (**Vh**).* Yellowish white solid (0.19 gm – 67%) mp = 206 °C; IR (KBr) cm^{-1}: 3321 (NH), 3088 (CH aromatic), 2954 (CH aliphatic), 1687 (C=O amide), 1644 (C=N); ^{1}H NMR (400 MHz, DMSO-d_6) δ: 12.16 (brs, 1H), 8.53 (s, 1H), 8.32 (s, 1H), 7.97 (s, 2H), 7.87 (d, J = 8 Hz, 1H), 7.77 (d, J = 8 Hz, 1H), 7.43 (s, 2H), 7.13 (s, 2H), 3.85 (s, 6H), 3.70 (s, 3H), 2.65 (s, 1H). ^{13}C NMR (100 MHz, DMSO) δ: 164.20, 160.12, 157.99, 153.10, 151.76, 148.92, 146.88, 144.44, 139.23, 138.92, 133.65, 131.60, 124.28, 118.77, 113.56, 104.51, 60.73, 56.56, 22.54; MS (*m*/*z*): 477 (0.4%, M + 2), 475 (0.8%, M + 2), 473 (1.2%, M^+); anal. calc. for: ($C_{23}H_{21}Cl_2N_3O_4$, M_{wt} = 473): C, 58.24; H, 4.46; N, 8.86; found: C, 58.32; H, 4.53; N, 8.97%.

*4.1.5.9. (E)-N′-[4-(Dimethylamino)benzylidene]-2-methyl-6-(3,4,5-trimethoxyphenyl)nicotinohydrazide (**Vi**).* Yellowish white solid (0.22 g – 79%) mp = 136 °C; IR (KBr) cm^{-1}: 3298 (NH), 3068 (CH aromatic), 2914 (CH aliphatic), 1688 (C=O amide), 1635 (C=N); ^{1}H NMR (400 MHz, DMSO-d_6) δ: 11.56 (brs, 1H), 8.13 (s, 1H), 7.94 (d, J = 8 Hz, 1H), 7.89 (d, J = 8 Hz, 1H), 7.54 (d, J = 8 Hz, 2H), 7.41 (s, 2H), 6.76 (d, J = 8 Hz, 2H), 3.87 (s, 6H), 3.71 (s, 3H), 2.97 (s, 6H), 2.63 (s, 1H). ^{13}C NMR (100 MHz, DMSO) δ: 167.75, 160.11, 156.25, 155.23, 153.10, 148.61, 139.24, 137.50, 132.31, 129.48, 128.45, 125.79, 121.84, 113.88, 104.52, 60.73, 56.25, 30.89, 23.24; MS (*m*/*z*) 448; anal. calc. for: ($C_{25}H_{28}N_4O_4$, M_{wt} = 448): C, 66.95; H, 6.29; N, 12.49; found: C, 67.04; H, 6.45; N, 12.36%.

*4.1.5.10. (E)-2-Methyl-N′-(4-nitrobenzylidene)-6-(3,4,5-trimethoxyphenyl)nicotinohydrazide (**Vj**).* Orange solid (0.16 g – 55%) mp = 241 °C; IR (KBr) cm^{-1}: 3311 (NH), 3082 (CH aromatic), 2923 (CH aliphatic), 1687 (C=O amide), 1630 (C=N); ^{1}H NMR (400 MHz, DMSO-d_6) δ: 12.19 (brs, 1H), 8.41 (s, 1H), 8.31 (d, J = 8 Hz, 2H), 8.20 (d, J = 8 Hz, 1H), 8.01 (d, J = 8 Hz, 1H), 7.99 (d, J = 8 Hz, 2H), 7.43 (s, 2H), 3.88 (s, 6H), 3.71 (s, 3H), 2.65 (s, 1H). ^{13}C NMR (100 MHz, DMSO) δ: 165.93, 163.18, 161.84, 158.68, 153.50, 149.63, 139.24, 138.22, 134.36, 129.87, 128.14, 124.67, 117.75, 116.32, 111.84, 60.73, 56.56, 23.64; MS (*m*/*z*) 450; anal. calc. for: ($C_{23}H_{22}N_4O_6$, M_{wt} = 450): C, 61.33; H, 4.92; N, 12.44; found: C, 61.17; H, 5.04; N, 12.58%.

*4.1.5.11. (E)-2-Methyl-N′-(pyridin-4-ylmethylene)-6-(3,4,5-trimethoxyphenyl)nicotinohydrazide (**Vk**).* White solid (0.16 g – 62%) mp = 221 °C; IR (KBr) cm^{-1}: 3333 (NH), 3069 (CH aromatic), 2974 (CH aliphatic), 1688 (C=O amide), 1628 (C=N); ^{1}H NMR (400 MHz, DMSO-d_6) δ: 12.15 (brs, 1H), 8.65 (d, J = 8 Hz, 2H), 8.30 (s, 1H), 8.0 (d, J = 8 Hz, 1H), 7.93 (d, J = 8 Hz, 1H), 7.67 (d, J = 8 Hz, 2H), 7.43 (s, 2H), 3.88 (s, 6H), 3.71 (s, 3H), 2.64 (s, 1H). ^{13}C NMR (100 MHz, DMSO) δ: 165.41, 163.22, 159.32, 157.87, 153.64, 150.77, 144.23, 139.55, 138.12, 133.67, 126.12, 120.83, 112.64, 104.16, 60.57, 56.49, 23.61; MS (*m*/*z*) 406; anal. calc. for: ($C_{22}H_{22}N_4O_4$, M_{wt} = 406): C, 65.01; H, 5.46; N, 13.78; found: C, 65.13; H, 5.59; N, 13.95%.

4.1.6. (3,5-Dimethyl-1*H*-pyrazol-1-yl)[2-methyl-6-(3,4,5-trimethoxyphenyl)pyridin-3-yl]methanone (VI). A solution of compound **IV** (0.2 g, 0.6 mmol) in 25 mL absolute ethanol was added to a solution of acetonyl acetone (0.06 g, 0.6 mmol) and 1 N glacial acetic acid (5 mL). The mixture was heated for 7 h and the progress of reaction was monitored using TLC. After completion, the reaction mixture was concentrated and poured in ice cold water (100–150 mL). The separated solid was filtered, washed with water and then recrystallized from ethanol to give compound **VI** as orange solid (0.2 g – 84%) mp = 197 °C; ^{1}H NMR (400 MHz, DMSO-d_6) δ: 8.20 (d, J = 8 Hz, 1H), 7.93 (d, J = 8 Hz, 1H), 7.42 (s, 2H), 6.61 (s, 1H), 3.85 (s, 6H), 3.70 (s, 3H), 2.77 (s, 1H), 2.09 (s, 3H), 2.06 (s, 3H). ^{13}C NMR (100 MHz, DMSO) δ: 172.61, 168.0, 158.89, 157.49, 153.60, 146.69, 139.68, 139.54, 133.57, 129.95, 124.55, 117.75, 104.62, 60.62, 56.44, 25.30, 21.44, 21.36; MS (*m*/*z*) 381; anal. calc. for: ($C_{21}H_{23}N_3O_4$, M_{wt} = 381): C, 66.13; H, 6.08; N, 11.02; found: C, 66.26; H, 6.24; N, 11.23%.

4.1.7. 5-[2-Methyl-6-(3,4,5-trimethoxyphenyl)pyridin-3-yl]-1,3,4-oxadiazole-2-thiol (VII). Potassium hydroxide (0.35 g, 8.5 mmol) was added to a solution of **IV** (2.7 g, 8.5 mmol) in 15 mL ethanol, followed by addition of carbon disulphide dropwise (2.5 mL, 93.5 mmol) over 0.5 h. The reaction mixture was stirred at room temperature for an additional 15 min and then heated to reflux until H_2S gas evolution was ceased. After completion of the reaction, as monitored by TLC, the obtained intermediate **VII** was poured on 50 mL cold water, filtered, washed with water, dried and crystallized from ethanol to give yellow crystals (2.7 g, 89%) mp > 300 °C; ^{1}H NMR (400 MHz, DMSO) δ: 8.19 (d, J = 8 Hz, 1H), 8.03 (d, J = 8 Hz, 1H), 7.44 (s, 2H), 3.84 (s, 6H), 3.70 (s, 3H), 2.79 (s, 3H); ^{13}C NMR (100 MHz, DMSO) δ: 167.36, 159.71, 156.57, 153.50, 139.56, 137.12, 133.01, 118.07, 116.33, 104.51, 60.42, 56.56, 25.37; MS (*m*/*z*) 359 (free base).

4.1.8. General procedure for synthesis of compounds (VIIIa–e). To a suspension of **VII** (3.59 g, 10 mmol) and

anhydrous sodium acetate (1.25 g, 15 mmol) in absolute ethanol (30 mL), the appropriate alkylhalide (10 mmol) was added. The reaction mixture was heated under reflux for 2 hours. After cooling down to room temperature, the precipitate was collected and recrystallized from absolute ethanol to provide the desired products.

*4.1.8.1. 2-[2-Methyl-6-(3,4,5-trimethoxyphenyl)pyridin-3-yl]-5-(methylthio)-1,3,4-oxadiazole (**VIIIa**).* Pale green solid (3.1 g – 82%) mp = 174 °C; ^{1}H NMR (400 MHz, DMSO-d_6) δ: 8.27 (d, J = 8 Hz, 1H), 8.06 (d, J = 8 Hz, 1H), 7.47 (s, 2H), 3.87 (s, 6H), 3.71 (s, 3H), 2.87 (s, 3H), 2.77 (s, 3H). ^{13}C NMR (100 MHz, DMSO) δ: 165.94, 164.59, 156.96, 156.25, 153.50, 139.24, 137.50, 133.33, 118.77, 116.63, 104.52, 60.42, 56.24, 25.69, 14.90; MS (*m*/*z*) 373; anal. calc. for: ($C_{18}H_{19}N_3O_4S$, M_{wt} = 373): C, 57.90; H, 5.13; N, 11.25; found: C, 58.06; H, 5.79; N, 11.42%.

*4.1.8.2. 2-(Ethylthio)-5-[2-methyl-6-(3,4,5-trimethoxyphenyl) pyridin-3-yl]-1,3,4-oxadiazole (**VIIIb**).* White solid (3.3 g – 86%) mp = 166 °C; ^{1}H NMR (400 MHz, DMSO-d_6) δ: 8.27 (d, J = 8 Hz, 1H), 8.06 (d, J = 8 Hz, 1H), 7.47 (s, 2H), 3.87 (s, 6H), 3.71 (s, 3H), 3.45 (m, 2H), 2.87 (s, 3H), 1.44 (t, J = 8 Hz, 3H). ^{13}C NMR (100 MHz, DMSO) δ: 167.74, 157.99, 154.52, 154.21, 152.79, 139.95, 137.83, 133.34, 121.53, 116.64, 104.82, 60.42, 56.56, 30.90, 25.38, 15.30; MS (*m*/*z*) 387; anal. calc. for: ($C_{19}H_{21}N_3O_4S$, M_{wt} = 387): C, 58.90; H, 5.46; N, 10.85; found: C, 59.07; H, 5.57; N, 11.03%.

*4.1.8.3. 2-[(3-Bromopropyl)thio]-5-[2-methyl-6-(3,4,5-trimethoxyphenyl)pyridin-3-yl]-1,3,4-oxadiazole (**VIIIc**).* Yellow solid (3.5 g – 73%) mp = 178 °C; ^{1}H NMR (400 MHz, DMSO-d_6) δ: 8.28 (d, J = 8 Hz, 1H), 8.07 (d, J = 8 Hz, 1H), 7.47 (s, 2H), 3.88 (s, 6H), 3.79 (t, J = 8 Hz, 2H), 3.71 (s, 3H), 3.44 (t, J = 8 Hz, 2H), 2.88 (s, 3H), 2.29 (p, J = 8 Hz, 2H). ^{13}C NMR (100 MHz, DMSO) δ: 164.91, 164.21, 156.96, 155.93, 153.81, 139.56, 137.83, 133.34, 118.38, 117.03, 104.51, 60.41, 56.56, 32.30, 30.88, 30.18, 25.69; MS (*m*/*z*) 480; anal. calc. for: ($C_{20}H_{22}BrN_3O_4S$, M_{wt} = 480): C, 50.01; H, 4.62; Br, 16.63; N, 8.75; found: C, 50.18; H, 4.76; N, 8.91%.

*4.1.8.4. 2-(Hexylthio)-5-[2-methyl-6-(3,4,5-trimethoxyphenyl) pyridin-3-yl]-1,3,4-oxadiazole (**VIIId**).* Yellow solid (3.6 g – 81%) mp = 157 °C; ^{1}H NMR (400 MHz, DMSO-d_6) δ: 8.26 (d, J = 8 Hz, 1H), 8.04 (d, J = 8 Hz, 1H), 7.45 (s, 2H), 3.86 (s, 6H), 3.70 (s, 3H), 3.31 (d, J = 8 Hz, 2H), 2.86 (s, 3H), 1.76–1.72 (m, 1H), 1.42–1.27 (m, 5H), 0.8–0.82 (m, 6H). ^{13}C NMR (100 MHz, DMSO) δ: 164.21, 157.98, 153.80, 153.50, 152.07, 140.26, 137.82, 133.32, 118.37, 116.32, 104.52, 60.59, 56.48, 31.06, 29.35, 27.87, 25.54, 22.28, 14.20; MS (*m*/*z*) 443; anal. calc. for: ($C_{23}H_{29}N_3O_4S$, M_{wt} = 443): C, 62.28; H, 6.59; N, 9.47; found: C, 62.47; H, 6.68; N, 9.65%.

*4.1.8.5. 2-[(Cyclohexylmethyl)thio]-5-[2-methyl-6-(3,4,5-trimethoxyphenyl)pyridin-3-yl]-1,3,4-oxadiazole (**VIIIe**).* Yellow solid (3.1 g – 68%) mp = 111 °C; ^{1}H NMR (400 MHz, DMSO-d_6) δ: 8.26 (d, J = 8 Hz, 1H), 8.04 (d, J = 8 Hz, 1H), 7.45 (s, 2H), 3.86 (s, 6H), 3.70 (s, 3H), 3.22 (d, J = 8 Hz, 2H), 2.85 (s, 3H), 1.83–1.55 (m, 5H), 1.20–0.98 (m, 6H). ^{13}C NMR (100 MHz, DMSO) δ: 164.81, 164.61, 156.97, 156.53, 153.52, 139.68, 137.72, 133.22, 118.10, 116.95, 104.84, 60.59, 56.48, 37.57, 31.97, 31.09, 26.06, 25.69, 25.49; MS (*m*/*z*) 455; anal. calc. for: ($C_{24}H_{29}N_3O_4S$, M_{wt} = 455): C, 63.28; H, 6.42; N, 9.22; found: C, 63.47; H, 6.51; N, 9.41%.

4.2. Biological assays

4.2.1. *In vitro* anti-proliferative activity. The *in vitro* anti-cancer screening including colorectal carcinoma (HCT-116), hepatocellular carcinoma (HepG-2) and breast cancer (MCF-7) for the synthesized compounds as well as colchicine as a control at various doses was applied using MTT assay.[29–32] Cell lines was brought from American Type Culture Collection. The plate cells were used (cells density 1.2–1.8 × 10 000 cells per well) where 100 μl of complete growth medium was added to 100 μl of each of the tested compounds per well of a 96-well plate and kept for 24 hours before MTT assay. The MTT method was applied with multiwell plates. Where final cell count didn't exceed 10^6 cells per cm^2. A blank containing only the medium without the cells was included for each test. Absorbance was measured using spectrophotometer at wavelength of 570 nm. The background absorbance being measured at 690 nm of multiwell plates was further subtracted from the 450 nm absorbance. Suitable plate reader and appropriate size cuvettes were used for spectrophotometric measurement.

4.2.2. *In vitro* tubulin polymerization assay. The tubulin polymerization effect of the synthesized compounds **Vb**, **Vc**, **Vd**, **Vf**, **Vj**, **Vk**, **VI**, **VIIIa**, **VIIIb** & **VIIId** was assessed turbidimetrically using a fluorescent plate reader method.[33]

4.2.3. Cell cycle analysis. The cell cycle analysis protocol was applied based on the quantitation of the amount of DNA stained by propidium iodide. Cells were first washed in PBS before being kept for 3 min at 4 °C by dropwise addition of cold 70% ethanol under vortex, to avoid cell clumping. Then ribonuclease was added (50 μl from a stock of 100 μg mL^{-1}) in order to confirm staining of DNA only. Then, (200 μl from a stock concentration of 50 μg mL^{-1}) of propidium iodide was added.[34–37]

4.2.4. Annexin V-FITC apoptosis assay. The assay depends on the translocation of phosphatidylserine (PS) after apoptosis initiation to the cell surface. Where PS can be stained using the high affinity protein fluorescent conjugate of annexin V. The staining test is completed in one-step within 10 minutes, then detection using flow cytometry is performed.

The effect of compound **VI** on apoptosis induction was investigated using annexin V-FITC/PI apoptosis detection kit.[38–40]

4.3. Molecular docking study

Molecular docking study was conducted using Libdock 4.0 protocol in Discovery Studio (DS 4.1 Biovia Discovery Studio 2016 64-bit Client), at Faculty of Pharmacy, Future University in Egypt-drug design laboratory. The enzyme tubulin complex with colchicine was downloaded from Protein Data Bank (PDB ID: 4O2B).[41]

Funding

No funding

Conflicts of interest

All the authors declare that they have no conflict of interest.

References

1 F. Xu, W. Li, W. Shuai, L. Yang, Y. Bi, C. Ma, H. Yao, S. Xu, Z. Zhu and J. Xu, *Eur. J. Med. Chem.*, 2019, **173**, 1–4.
2 J. Howard and A. A. Hyman, *Nature*, 2003, **422**, 753–758.
3 M. A. Jordan and L. Wilson, *Nat. Rev. Cancer*, 2004, **4**, 253–265.
4 S. Liu, M. Gao, L. Wang, J. Sun, J. Du, Q. Guan, K. Bao, D. Zuo, Y. Wu and W. Zhang, *Eur. J. Med. Chem.*, 2019, **168**, 426–435.
5 C. Dumontet and M. A. Jordan, *Nat. Rev. Drug Discovery*, 2010, **10**, 790–803.
6 M. Hagras, M. A. El Deeb, H. S. Elzahabi, E. B. Elkaeed, A. B. Mehany and I. H. Eissa, *J. Enzyme Inhib. Med. Chem.*, 2021, **36**, 640–658.
7 M. A. Jordan and K. Kamath, *Curr. Cancer Drug Targets*, 2007, **7**, 730–742.
8 Y. Lu, J. Chen, M. Xiao, W. Li and D. D. Miller, *Pharm. Res.*, 2012, **29**, 2943–2971.
9 A. Jordan, J. A. Hadfield, N. J. Lawrence and A. T. McGown, *Med. Res. Rev.*, 1998, **18**, 259–296.
10 P. Giannakakou, D. Sackett and T. Fojo, *J. Natl. Cancer Inst.*, 2000, **92**, 182–183.
11 P. M. Checchi, J. H. Nettles, J. Zhou, J. P. Snyder and H. C. Joshi, *Trends Pharmacol. Sci.*, 2003, **24**, 361–365.
12 E. Porcù, R. Bortolozzi, G. Basso and G. Viola, *Future Med. Chem.*, 2014, **6**, 1485–1498.
13 S. D. Guggilapu, L. Guntuku, T. S. Reddy, A. Nagarsenkar, D. K. Sigalapalli, V. G. Naidu, S. K. Bhargava and N. B. Bathini, *Eur. J. Med. Chem.*, 2017, **138**, 83–95.
14 B. S. Kumar, A. Kumar, J. Singh, M. Hasanain, A. Singh, K. Fatima, D. K. Yadav, V. Shukla, S. Luqman, F. Khan and D. Chanda, *Eur. J. Med. Chem.*, 2014, **86**, 740–751.
15 M. M. Abdelshaheed, I. M. Fawzy, H. I. El-Subbagh and K. M. Youssef, *Future Journal of Pharmaceutical Sciences*, 2021, **7**, 1–11.
16 E. A. Mohamed, N. S. Ismail, M. Hagras and H. Refaat, *Future Journal of Pharmaceutical Sciences*, 2021, **7**, 1–7.
17 S. Zheng, Q. Zhong, M. Mottamal, Q. Zhang, C. Zhang, E. LeMelle, H. McFerrin and G. Wang, *J. Med. Chem.*, 2014, **57**, 3369–3381.
18 R. Pettit George, M. Cragg Gordon, L. Herald Delbert and M. Schmidt Jean, *Can. J. Chem.*, 1982, **60**, 1374–1376.
19 G. R. Pettit, C. Temple Jr, V. L. Narayanan, R. A. Varma, M. J. Simpson, M. R. Boyd, G. A. Rener and N. A. Bansal, *Anti-Cancer Drug Des.*, 1995, **10**, 299–309.
20 R. B. Ravelli, B. Gigant, P. A. Curmi, I. Jourdain, S. Lachkar, A. Sobel and M. Knossow, *Nature*, 2004, **428**, 198–202.
21 R. Gaspari, A. E. Prota, K. Bargsten, A. Cavalli and M. O. Steinmetz, *Chem*, 2017, **2**, 102–113.
22 W. Li, H. Sun, S. Xu, Z. Zhu and J. Xu, *Future Med. Chem.*, 2017, **9**, 1765–1794.
23 Z. Wang, J. Chen, J. Wang, S. Ahn, C. M. Li, Y. Lu, V. S. Loveless, J. T. Dalton, D. D. Miller and W. Li, *Pharm. Res.*, 2012, **29**, 3040–3052.
24 Q. X. Yue, X. Liu and D. A. Guo, *Planta Med.*, 2010, **76**, 1037–1043.
25 X. Wu, Q. Wang and W. Li, *Curr. Med. Chem.: Anti-Cancer Agents*, 2016, **16**, 1325–1338.
26 M. Dong, F. Liu, H. Zhou, S. Zhai and B. Yan, *Molecules*, 2016, **21**, 1375.
27 D. M. Patterson and G. J. Rustin, *Clin. Oncol.*, 2007, **19**, 443–456.
28 E. Hoggarth, *J. Chem. Soc.*, 1952, 4811–4817.
29 N. E. Abd El-Sattar, E. H. Badawy, W. H. AbdEl-Hady, M. I. Abo-Alkasem, A. A. Mandour and N. S. Ismail, *Chem. Pharm. Bull.*, 2021, **69**, 106–117.
30 M. I. Thabrew, R. D. Hughes and I. G. McFarlane, *J. Pharm. Pharmacol.*, 1997, **49**, 1132–1135.
31 T. Mosmann, *J. Immunol. Methods*, 1983, **65**, 55–63.
32 F. Denizot and R. Lang, *J. Immunol. Methods*, 1986, **89**, 271–277.
33 G. M. Morris, D. S. Goodsell, R. S. Halliday, R. Huey, W. E. Hart, R. K. Belew and A. J. Olson, *J. Comput. Chem.*, 1998, **19**, 1639–1662.
34 P. Pozarowski and Z. Darzynkiewicz, in *Checkpoint Controls and Cancer*, Humana Press, 2004, pp. 301–311.
35 J. Wang and M. J. Lenardo, *J. Cell Sci.*, 2000, **113**, 753–757.
36 T. Al-Warhi, M. F. Abo-Ashour, H. Almahli, O. J. Alotaibi, M. M. Al-Sanea, G. H. Al-Ansary, H. Y. Ahmed, M. M. Elaasser, W. M. Eldehna and H. A. Abdel-Aziz, *J. Enzyme Inhib. Med. Chem.*, 2020, **35**, 1300–1309.
37 W. M. Eldehna, A. Nocentini, Z. M. Elsayed, T. Al-Warhi, N. Aljaeed, O. J. Alotaibi, M. M. Al-Sanea, H. A. Abdel-Aziz and C. T. Supuran, *ACS Med. Chem. Lett.*, 2020, **11**, 1022–1027.
38 K. K. Lo, T. K. Lee, J. S. Lau, W. L. Poon and S. H. Cheng, *Inorg. Chem.*, 2008, **47**, 200–208.
39 A. Sabt, W. M. Eldehna, T. Al-Warhi, O. J. Alotaibi, M. M. Elaasser, H. Suliman and H. A. Abdel-Aziz, *J. Enzyme Inhib. Med. Chem.*, 2020, **35**, 1616–1630.
40 W. M. Eldehna, G. S. Hassan, S. T. Al-Rashood, T. Al-Warhi, A. E. Altyar, H. M. Alkahtani, A. A. Almehizia and H. A. Abdel-Aziz, *J. Enzyme Inhib. Med. Chem.*, 2019, **34**, 322–332.
41 A. E. Prota, F. Danel, F. Bachmann, K. Bargsten, R. M. Buey, J. Pohlmann, S. Reinelt, H. Lane and M. O. Steinmetz, *J. Mol. Biol.*, 2014, **426**, 1848–1860.